Chapter 27
LEAP-UCD-2017 Simulation Team Fugro

Dimitra Tsiaousi, Jose Ugalde, and Thaleia Travasarou

Abstract Fugro participated in the Liquefaction Experiment and Analysis Projects (LEAP) by performing numerical simulations using two different constitutive models implemented in the software FLAC. Fugro developed a calibration framework based on soil-specific laboratory test data considering multiple elements of dynamic response such as liquefaction triggering criteria (i.e., number of cycles to a specified strain and pore pressure ratio threshold) as well as post-triggering strain accumulation rate. The calibrated model parameters were subsequently used to obtain "Type B (blind)" predictions of the centrifuge experiments with the opportunity to refine after the centrifuge results were provided (Type C simulations). Overall, Fugro's blind predictions captured the centrifuge test responses well with small refinements needed during Type C simulations. Estimated deformations were within a factor of about two compared to the observed. The overall good comparison provides confidence in the proposed calibration framework, which can be implemented and used for different sand types and project conditions.

27.1 Introduction

The LEAP 2017 simulation exercise consisted of the following four stages: (1) constitutive model calibration, (2) Type-B (blind) predictions, (3) Type-C simulations, and (4) sensitivity analyses. A series of stress-controlled cyclic triaxial laboratory tests were available (El Ghoraiby et al. 2017, 2019) and used in the calibration process. Next, the model parameters obtained during model calibration were used to analyze the centrifuge experiments, providing the base excitation and the soil density without any knowledge of the actual results (Type-B predictions). The simulation teams were subsequently provided with the centrifuge experiment results and simulations were refined, if necessary, to obtain better agreement (Type-C simulations).

D. Tsiaousi (✉) · J. Ugalde · T. Travasarou
Fugro, Walnut Creek, CA, USA
e-mail: dtsiaousi@fugro.com

B. Kutter et al. (eds.), *Model Tests and Numerical Simulations of Liquefaction and Lateral Spreading*, https://doi.org/10.1007/978-3-030-22818-7_27

Last, a series of sensitivity analyses were performed to assess the influence of soil relative density (D_R), motion intensity, and motion high frequency content on the simulation results.

27.2 Constitutive Model Calibration

27.2.1 Introduction

Fugro calibrated two constitutive models, PM4SAND and UBCSAND, to the available cyclic stress-controlled triaxial laboratory tests on Ottawa F65 sand (El Ghoraiby et al. 2017, 2019). The cyclic triaxial tests were performed for three different soil densities. The three groups of specimens tested had void ratios of approximately 0.585, 0.542, and 0.515 corresponding to relative densities of about 65%, 80%, and 90%, respectively, based on a maximum void ratio (e_{max}) of 0.74 and a minimum void ratio (e_{min}) of 0.49 per Vasko as tabulated in Table 6 of the El Ghoraiby et al. (2017) report. At the time of this calibration process, no other test data was available.

Constitutive model calibration was performed considering multiple elements of response such as number of cycles to specified strain and pore pressure ratio thresholds as well as post-triggering strain accumulation rate.

27.2.2 Model Description, Parameters, and Implementation

PM4SAND Constitutive Model

PM4SAND Version 3 constitutive model developed by Boulanger and Ziotopoulou (2015) was initially calibrated. Stress-controlled plane strain compression (PSC) test simulations were performed using PM4SAND and calibrated against the available stress-controlled triaxial test data. The soil elements were initially confined with vertical and horizontal stresses of one atmosphere, considering coefficient of earth pressures at rest of one ($K_o = 1$). Plane strain compression loading conditions were stress controlled by imposing a velocity until a specific stress ratio was reached and then the sign of velocity was changed.

The model parameters are grouped into two categories: a primary and a secondary set of parameters that may be modified from their default values in special circumstances. The three primary input parameters are the sand's apparent relative density D_R, the shear modulus coefficient G_o, and the contraction rate parameter h_{po}. The contraction rate parameter h_{po} was used to calibrate the liquefaction triggering resistance, and the shear modulus parameter G_o was mainly used to calibrated the strain rate accumulation. PM4SAND calibrated model parameters are tabulated in Table 27.1. A detailed description of the primary and secondary input parameters

Table 27.1 PM4SAND calibrated model parameters

Parameter	Function	Values
D_R	Relative density	65%, 80%, and 90% for e_o of 0.585, 0.542, and 0.515, respectively based on $e_{max} \sim 0.74$ and $e_{min} \sim 0.49$
G_o	Shear modulus coefficient	625, 1321, and 2001 for void ratio e_o of 0.585, 0.542, and 0.515, respectively based on the equation: $G_o = 167 \times (N_{1,60} + 2.5)^{0.5}$ and using multiplier of 0.8, 1.4, and 1.9 for e_o of 0.585, 0.542, and 0.515, respectively
h_{po}	Contraction rate parameter	0.07, 0.038, and 0.03 for void ratio e_o of 0.585, 0.542, and 0.515, respectively
e_{max} and e_{min}	Maximum and minimum void ratios	$e_{max} \sim 0.74$ and $e_{min} \sim 0.49$ based on lab test data per Table 6 of the El Ghoraiby et al. (2017) report

and default values is provided in Tables 4.1 and 4.2 in Boulanger and Ziotopoulou (2015).

Plane strain compression tests were simulated for the relative densities of 65%, 80%, and 90% for various cyclic stress ratios (CSR) in order to compare the plane strain simulation results with the triaxial test results. Each plane strain compression simulation was compared to a triaxial test of a soil sample with similar relative density and stress ratio (CSR) in terms of liquefaction triggering and strain accumulation rate. Liquefaction strength curves were plotted for both the actual triaxial tests and the simulated plane strain compression tests in terms of numbers of cycles to 98% excess pore pressure ratio, and 2 and 5% double amplitude axial strain.

Figure 27.1 presents the observed (from the tests—red) and simulated (with calibrated soil properties—blue) liquefaction strength curve for the case of sand with D_R of 65%. Figure 27.2 presents the observed and simulated response in terms of (a) deviatoric stress versus mean effective stress, (b) deviatoric stress versus axial strain, (c) mean effective stress versus axial strain, and (d) pore pressure ratio versus number of cycles for all the plane strain compression simulations and superimposed with the respective triaxial tests for comparison purposes for the case of D_R of 65% and CSR of 0.2.

The constitutive model was also calibrated based on the average axial strain accumulation rate (SAR). SAR is defined in units of percent of strain per cycle and indicates the half double-amplitude strain accumulation per cycle (average of triaxial extension and compression) after liquefaction triggering. Figure 27.3 presents a comparison of SAR observed during the triaxial tests and that from the simulations using the calibrated parameters for PM4SAND for the case of D_R of 65%. For the PSC simulations, the strain accumulation rate (SAR) increases consistently with larger CSR. However, this trend is not consistent in the actual triaxial tests. Given this discrepancy, our goal was to approximate the average rate of SAR for CSR values between 0.14 and 0.2, which would be more relevant for the subsequent centrifuge tests. The observed versus simulated average rate of strain accumulation over these CSR values are 0.39% versus 0.42% strain per cycle, which are relatively in good agreement.

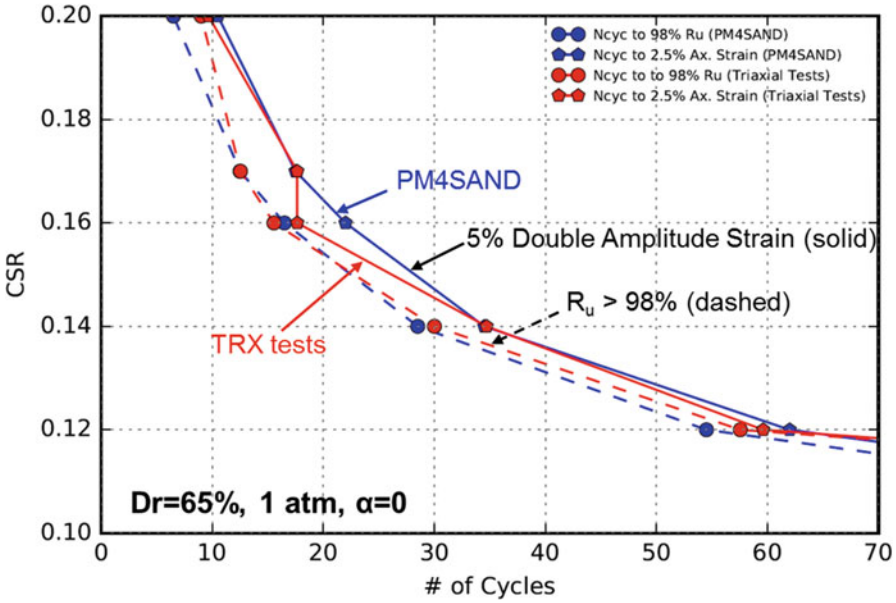

Fig. 27.1 Liquefaction strength curve for $D_R \sim 65\%$: triaxial test data versus plane strain compression simulation results using PM4SAND

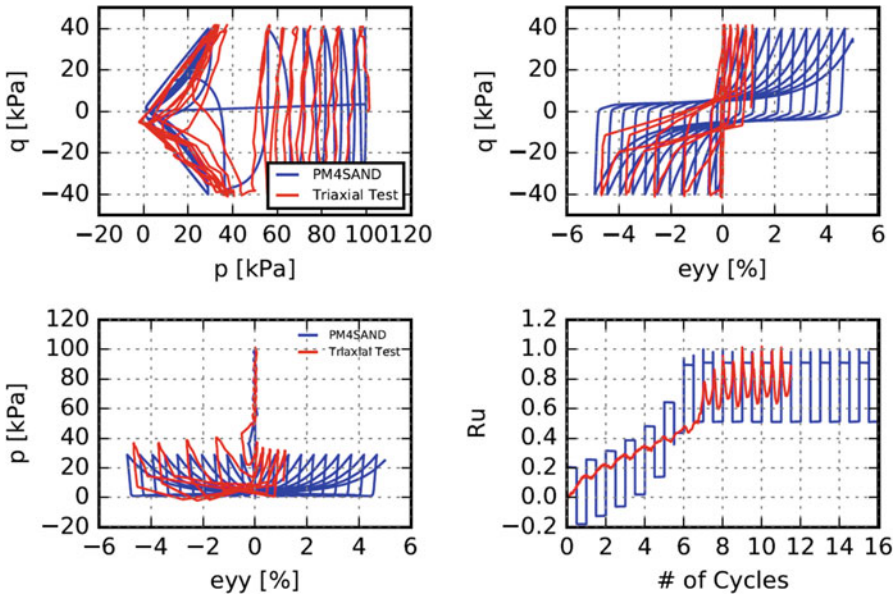

Fig. 27.2 Deviatoric stress versus mean effective stress, deviatoric stress versus axial strains, mean effective stress versus axial strains and pore pressure ratio versus number of cycles for $D_R \sim 65\%$ and CSR = 0.2, triaxial test data versus plane strain compression simulation using PM4SAND

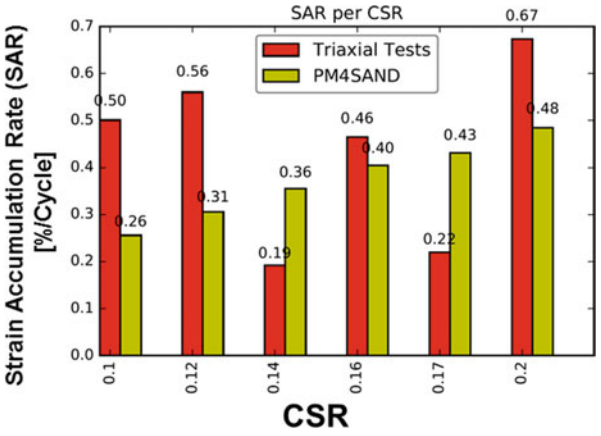

Fig. 27.3 Strain accumulation rate [%Strain/Ncyc] for $D_R \sim 65\%$ and different CSR values, triaxial test data versus plane strain compression simulation using PM4SAND—calibration process example

UBCSAND Constitutive Model

The UBCSAND constitutive model, which has been modified from the commonly available 904ar version by Fugro and Peter Burn, was also used in this study. This model has been modified, subsequently calibrated and validated by Fugro (Giannakou et al. 2011), and used in major projects such as the BART Offshore Transbay Tube Seismic Retrofit (Travasarou et al. 2011). The primary modification consists of introducing one additional model parameter (hfac4), which controls the rate of shear strain accumulation after liquefaction triggering. Detailed description of the model can be found in Beaty and Byrne (1998) and Byrne et al. (2004).

The model is fully defined by means of nine elastic and plastic parameters that can generally capture the observed response from monotonic and cyclic tests. Apart from $N_{1,60}$ which is a physical property of sand, four model parameters (hfac1 to hfac4; plastic hardeners) which are not related to physical properties are available to allow model calibration to observed behavior of different sands. Among these four parameters, the first three control the triggering of liquefaction (primarily the first two) while the fourth controls the post-trigger response. Table 27.2 summarizes the UBCSAND calibrated model parameters.

For calibration of the UBCSAND constitutive model, undrained cyclic direct simple shear (DSS) single element tests were simulated and compared against the DSS simulations using the PM4SAND calibrated properties. The UBCSAND model was not directly calibrated against the triaxial tests due to time limitations.

Liquefaction strength curves in terms of number of cycles to 98% pore pressure ratio, 1% shear strain, and 3% shear strain were compared against the cyclic simple shear simulations with the calibrated PM4SAND parameters. Figure 27.4 presents liquefaction strength curves for sand with D_R of 65%. Plots of CSR versus normalized vertical effective stress, CSR versus shear strain, normalized vertical effective stress versus shear strain, and pore pressure ratio versus number of cycles are also provided in Fig. 27.5. For comparison purposes, the results from the cyclic DSS simulations using PM4SAND with the calibrated parameters are superimposed with

Table 27.2 UBCSAND calibrated model parameters

Parameter	Function	Values
$N_{1,60}$	Normalized and corrected SPT Blowcount	19, 29, and 37 for D_R of 65%, 80%, and 90%, respectively
KGE	Elastic shear modulus multiplier	1166, 1339, and 1448 for D_R of 65%, 80%, and 90%, respectively based on the equation: $KGE = 21.7 \times 20 \times (N_{1,60})^{0.333}$
me	Elastic shear exponent	0.5
KB	Elastic bulk modulus multiplier	816, 937, and 1013 for D_R of 65%, 80%, and 90%, respectively based on the equation: $KB = KGE \times 0.7$
ne	Elastic bulk exponent	0.5
KGP	Plastic bulk modulus multiplier	1421, 3581, and 6130 for D_R of 65%, 80%, and 90%, respectively based on the equation: $KGP = KGE \times (N_{1,60})^2 \times 0.003 + 100.0$
np	Plastic bulk exponent	0.4
ϕ_{cs} (degrees)	Critical state friction angle	33
ϕ_{peak} (degrees)	Peak friction angle	36.9, 38.9, and 40.5 for D_R of 65%, 80%, and 90%, respectively
R_f	Failure ratio	0.81, 0.71, and 0.63 for D_R of 65%, 80%, and 90%, respectively
hfac1	Controls liquefaction triggering	0.45
hfac2	Controls liquefaction triggering	0.5
hfac3	Controls liquefaction triggering	1.0
hfac4	Controls post-trigger response	2.2, 2.0, and 1.8 for D_R of 65%, 80%, and 90%, respectively

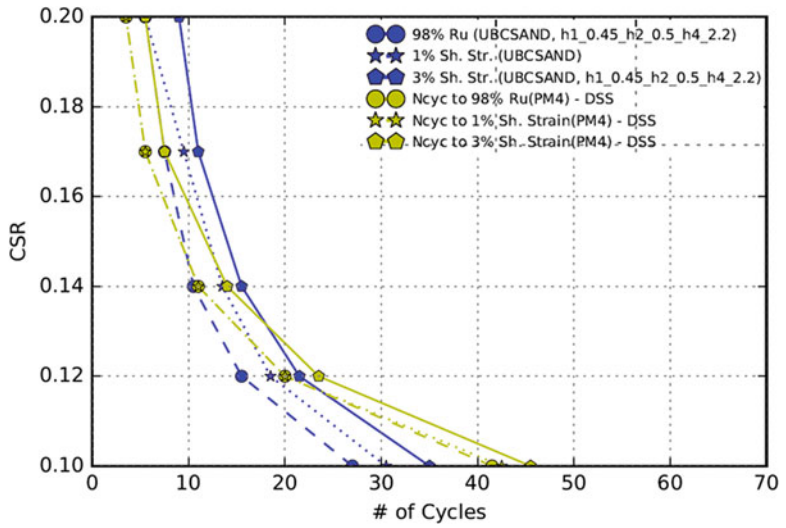

Fig. 27.4 Liquefaction strength curve in DSS conditions for $D_R \sim 65\%$, and cyclic direct simple shear simulations using PM4SAND and UBCSAND versus triaxial test data and plane strain compression simulations using PM4SAND

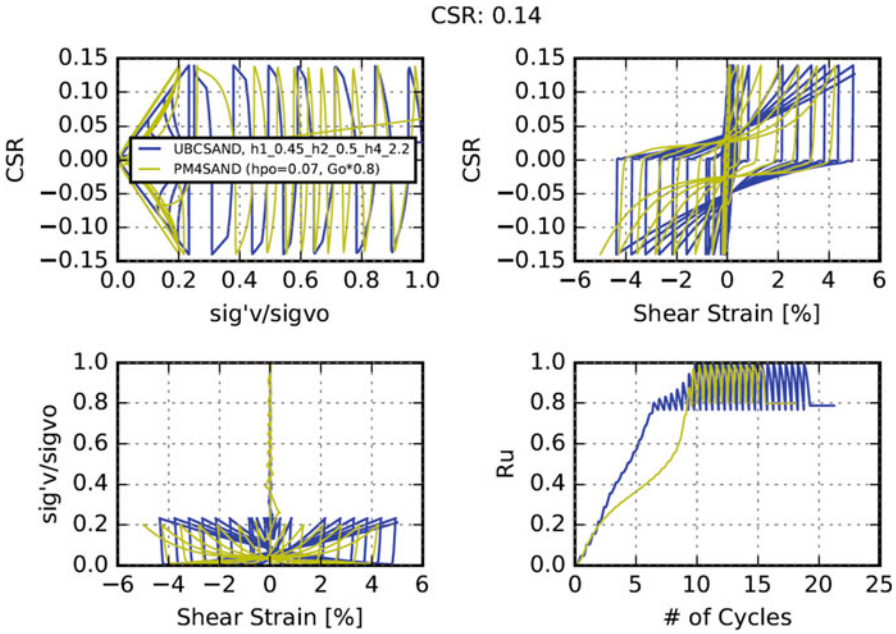

Fig. 27.5 CSR versus normalized vertical effective stress, CSR versus shear strain, normalized vertical effective stress versus shear strain and excess pore pressure ratio versus number of cycles for $D_R \sim 65\%$ and CSR = 0.14, DSS simulations using PM4SAND and UBCSAND

the results from the DSS simulations using UBCSAND with the calibrated parameters.

Overall, the liquefaction strength curves implied by UBCSAND are generally steeper than those implied by PM4SAND and the laboratory tests. Hence, the UBCSAND model may need to be calibrated with a tighter target CSR range, corresponding to that induced by the input motions.

27.3 Type B Simulations (Blind Predictions)

27.3.1 Introduction

During this phase of the project, the model parameters obtained as part of the calibration process were used to simulate the centrifuge experiments. The numerical simulations were conducted without any knowledge of the actual results. The simulation teams were only given information about the main characteristics of the centrifuge experiments, including the geometry of the centrifuge model, the

Table 27.3 Summary of centrifuge experiments selected for LEAP-2017 Type-B simulations

Experiment	Cent. Acc. (g)	μ/g	ρ_d (kg/m^3)	D_R (%)
CU-2	40	1.175	1605.8	46
Ehime-2[a]	40	1	1656.55	64
KAIST-1[a]	40	0.897	1701.2	78
KAIST-2	40	0.936	1592.5	42
KyU-3	44.4	0.991	1637	57
NCU-3[a]	26	1	1652	62
UCD-1[a]	43	1	1665	67
UCD-3[a]	43	1	1658	64
ZJU-2[a]	30	1	1606	46

[a]Selected subset of centrifuge tests considered for Type-B simulations

centrifugal acceleration, the viscosity of the pore fluid (μ), the base excitation (horizontal and vertical components) and the achieved soil density.

Nine centrifuge experiments were selected by the organizing committee for LEAP-2017 Type-B simulations. The main characteristics of these experiments such as the centrifugal acceleration in g, the ratio of the pore fluid viscosity over the gravity (μ/g), and the achieved dry soil density (ρ_d) are summarized in Table 27.3 This table also contains the relative density (D_R) which is calculated for each test according to Eq. 27.1:

$$D_R = \left(\frac{1/\rho_{d,min} - 1/\rho_d}{1/\rho_{d,min} - 1/\rho_{d,max}} \right) \tag{27.1}$$

where $\rho_{d,min}$ and $\rho_{d,min}$ are considered equal to 1485 and 1773 kg/m^3, respectively based on the average values of LEAP-2017 laboratory data on Ottawa F65 sand (El Ghoraiby et al. 2017). Six centrifuge experiments were selected by Fugro to be simulated at this phase due to time limitations: Tests Ehime-2, NCU-3, UCD-1, and UCD-3 with a relative density (D_R) of approximately 65%, test KAIST-1 with a D_R of approximately 80%, and test ZJU-2 with a D_R of approximately 50%.

27.3.2 Analysis Platform

The analysis platform used for the numerical simulation of the centrifuge experiments is FLAC2D, Version 7.0 for PM4Sand and Version 8.0 for UBCSAND, respectively (Itasca 2011, 2017). FLAC is a two-dimensional explicit finite difference program for engineering mechanics computation, following a "mixed discretization" scheme (Marti and Cundall 1982).

27.3.3 Numerical Modeling

Numerical modeling in FLAC was performed at the prototype scale. The model is 20 m long and 4 m high at the centerline. The soil surface forms a 5-degree slope. A horizontal ground water table with coordinates (−10, 0.875) and (10, 0.875) was assumed so that the slope is submerged. A baseline schematic of the centrifuge in prototype scale, illustrating the locations of pore pressure transducers, accelerometers and prescribed locations of displacement measurements, is presented in Fig. 27.6a. The grid and its dimensions of the numerical model are shown in Fig. 27.6b. The grid was built so that the grid points correspond to the locations of the accelerometers and the pore water pressure sensors illustrated in Fig. 27.6a.

A triangular pressure was applied at the soil surface simulating the load due to the water mass. Initially, during the gravity loading, Mohr-Coulomb properties were assigned to soil. A gravitational field with a vertical acceleration equal to 9.81 m/s^2 was applied and once equilibrium was reached, PM4SAND or UBCSAND constitutive models were assigned to soil elements and equilibrium was reached again. In the next step, the groundwater flow mode was set on and equilibrium was reached once more. During this process of gravity loading, the error tolerance was on the order of 10^{-4}. The pore pressure was fixed at the soil surface. The horizontal displacement was also fixed at the vertical boundaries of the model. Last, the base of the model was constrained to move neither horizontally nor vertically.

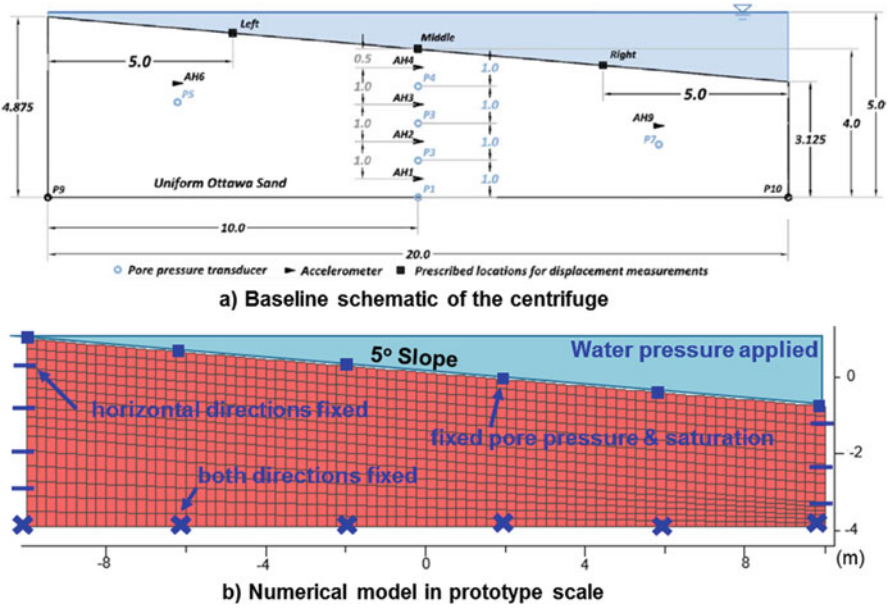

Fig. 27.6 (**a**) Baseline schematic of the centrifuge experiments, (**b**) Grid, model geometry, and boundary conditions used for numerical simulations of centrifuge experiments

After the end of the gravity loading phase, horizontal and vertical mean input motions, obtained from recorders AH11–12 and AV1–2, respectively, were applied at the base and the vertical boundaries of the model. Rayleigh damping (stiffness- and mass-proportional) with a minimum value of 0.5% at 3.3 Hz was assigned to the soil elements. After the end of shaking, the analyses continued until the excess pore water pressures dissipated fully. This procedure was followed for each of the simulated centrifuge tests. For each simulation, the corresponding input motions were baseline corrected and then applied to the model.

27.3.4 Material Properties and Constitutive Model Parameters

The material properties assumed in the numerical simulations, such as permeability, the water bulk modulus, the soil relative density and the dry soil density, are given in Table 27.4. These model properties were adopted following sensitivity analyses evaluating the effect of changes in water bulk modulus, permeability anisotropy, and Raleigh damping.

After shaking, the model was allowed to reconsolidate until excess pore pressures dissipated and initial effective stresses were re-established. After end of shaking, permeability was scaled by ten to reduce calculation time, and the time was also scaled in the post-processing phase to ensure that the results are not affected compared to the solutions that would have been obtained by not scaling the permeability.

As aforementioned, the gravity loading was applied in two stages. In the first stage, Mohr-Coulomb properties were assigned to the soil elements. Basically, the gravity loading was initially applied elastically since no failure occurred.

In the second stage of gravity loading, as well as the dynamic part of the numerical analyses, advanced constitutive models were assigned to the soil elements, such as PM4SAND and UBCSAND models. Constitutive models PM4SAND and UBCSAND were calibrated for soil relative densities of 65%, 80%, and 90%. For the Type-B simulations of centrifuge tests with D_R of about 65% (Ehime-2, NCU-3, UCD-1, and UCD-3) and 80% (KAIST-1), the initial calibrated parameters for a D_R of 65% and 80% were used, respectively. There

Table 27.4 Material properties used for numerical simulations

Centrifuge test	Permeability (cm/s)	Water bulk modulus (kPa)	D_R (%)	ρ_d (kg/m^3)
Ehime-2	0.0118	480,000	65	1657
NCU-3				1652
UCD-1				1665
UCD-3				1658
KAIST-1			80	1701
ZJU-2			50	1606

was no calibration performed for a D_R of 50%; hence, for Type-B simulation of ZJU-2 with a D_R of about 50%, the calibrated parameters corresponding to a D_R of 65% were used while a D_R of 50% was used as input to the simulation. For PM4SAND and UBCSAND constitutive models, the calibrated model parameters presented in Tables 27.1 and 27.2, respectively, were used based on the idealized relative density of each centrifuge test per Table 27.4.

27.3.5 Simulation Results

Figure 27.7 illustrates a comparison of the horizontal displacement and excess pore pressure ratio time histories at the middle surface of the model for Type-B simulation results using constitutive models UBCSAND, and PM4SAND versus Ehime 2 centrifuge experiment results. Both constitutive models and the centrifuge test results developed excess pore pressure ratio in excess of 80% while the rate of excess pore pressure dissipation recorded in the centrifuge is bounded by the two constitutive model predictions. Figure 27.8 presents a comparison of permanent horizontal displacement at the middle surface of the numerical models for Type-B simulation results using PM4SAND and UBCSAND versus the centrifuge experiment results for all cases simulated. Simulations with PM4SAND result in displacements closer to those measured and within a factor of 2 from the actual measurements with the exception of NCU3. Simulations with UBCSAND resulted in generally larger displacements than the actual measurements by a factor of about 2. This is likely attributed to the model calibration which was initially targeted at larger CSR ranges compared to those induced on average by the input ground motions. Overall, the blind predictions captured the centrifuge tests' behavior well and bounded the centrifuge response in most cases, indicating the benefits of using more than one constitutive model when performing numerical modeling.

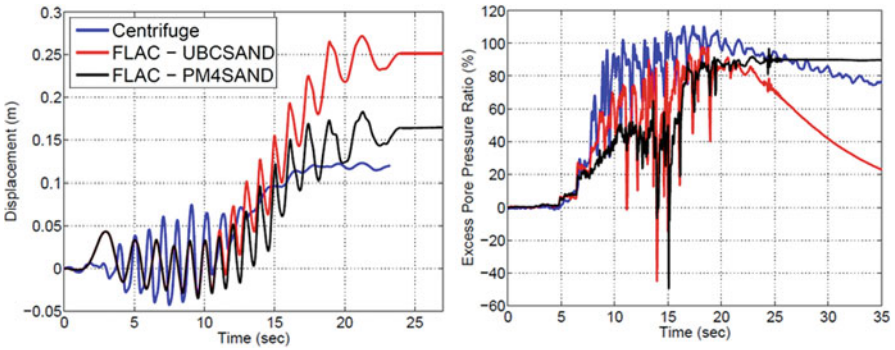

Fig. 27.7 Comparison of horizontal displacement and excess pore pressure ratio time histories at the middle surface of the model for Type-B simulation results using PM4SAND and UBCSAND versus Ehime 2 centrifuge experiment results

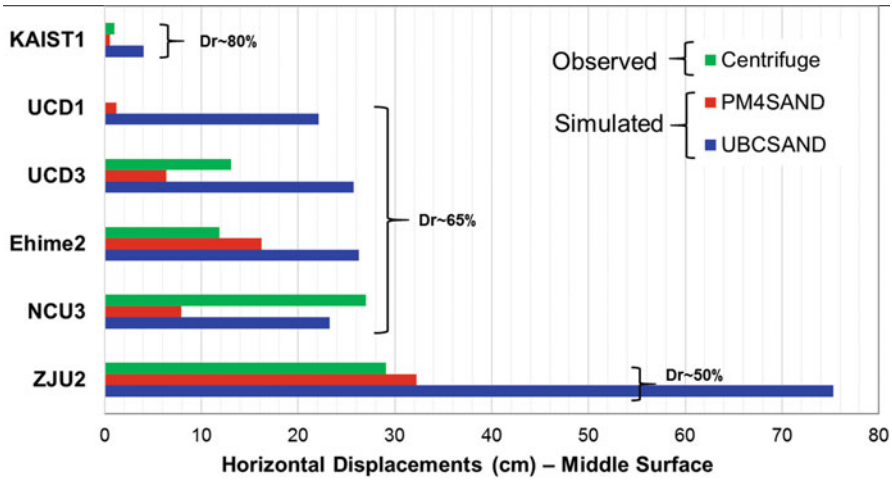

Fig. 27.8 Comparison of permanent horizontal displacement at the middle surface of the model for Type-B simulation results using PM4SAND and UBCSAND versus centrifuge experiment results for all cases simulated

27.4 Type-C Simulations

27.4.1 Introduction and Constitutive Model Parameters

At this stage, the centrifuge experiment results were released to the teams who were provided with the opportunity to refine the simulations, if necessary. In the Type-C simulations, the UBCSAND constitutive model parameters hfac1 and hfac2 were increased by 40% (hfac1 = 0.45 × 1.4 = 0.63 & hfac2 = 0.5 × 1.4 = 0.7) and the rest of the parameters are the same with the ones presented in Table 27.2. The PM4SAND constitutive model parameters were not modified and are the same with the ones presented in Table 27.1. As discussed before, the liquefaction strength curves implied by the UBCSAND model are steeper than the ones implied by PM4SAND and the laboratory tests. Hence, the UBCSAND model had to be recalibrated for a specific CSR range. Figure 27.9 illustrates the liquefaction strength curves from DSS simulations at a vertical effective stress of 0.2 atm for constitutive models PM4SAND (red) and UBCSAND using Type-B (blue) and Type-C (cyan) calibration parameters.

27.4.2 Simulation Results

Recalibrating UBCSAND constitutive model parameters resulted in permanent displacements closer to the actual measurements. Figure 27.10 illustrates a

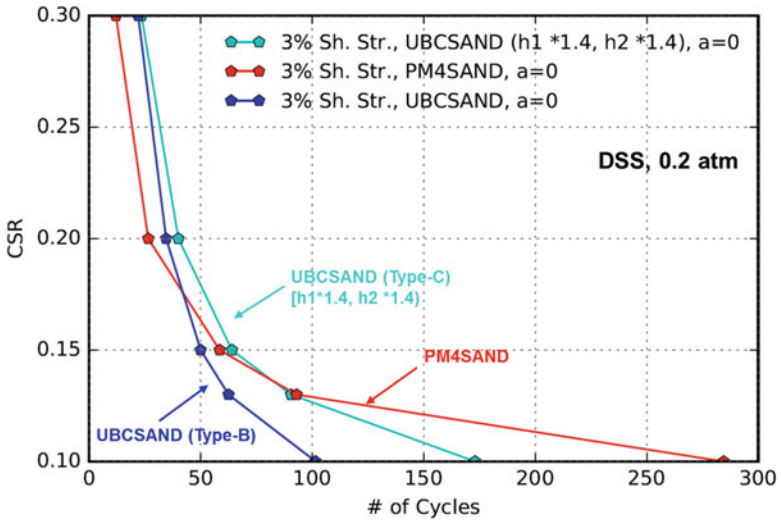

Fig. 27.9 Liquefaction strength curve for $D_R \sim 65\%$ and normal effective stress of 0.2 atm, direct simple shear simulations for PM4SAND and UBCSAND using calibration parameters from Type-B and Type-C calibrations

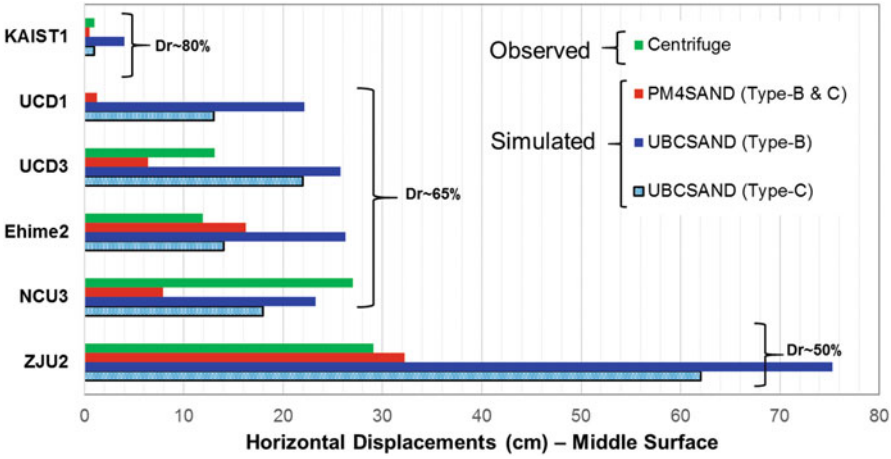

Fig. 27.10 Comparison of permanent horizontal displacement at the middle surface of the model for Type-B and Type-C simulation results using PM4SAND and UBCSAND versus centrifuge experiment results for all cases simulated

comparison of permanent horizontal displacement at the middle surface of the model for Type-B and Type-C simulation results for all cases simulated. The permanent displacements predicted from both constitutive models are within a factor of 2 from the actual measurements.

27.5 Sensitivity Study

27.5.1 Introduction

A sensitivity analysis study was performed to illustrate the sensitivity of the simulations to key input parameters such as relative density, ground motion intensity and the influence of superimposed high frequencies in the ground motions. The properties of the seven sensitivity analyses (NS-1 to NS-7) are tabulated in Table 27.5. All sensitivity analyses were performed using the constitutive model parameters that were used in Type-C simulations discussed in the previous section. Simulations NS-1, NS-4, NS-5, NS-6, and NS-7 with soil relative density of 65% were performed using the Type-C calibrated parameters for the case of D_R of 65%. Simulation NS-2 was performed using the Type-C calibrated parameters for the case of D_R of 65% but using as input a D_R of 50%. Simulation NS-3 was performed using the Type-C calibrated parameters for the case of D_R of 80% but using as input a D_R of 75%.

27.5.2 Sensitivity Analyses Results

Sensitivity analyses NS-1 to NS-3 were used to explore the sensitivity of simulations to relative density. Sensitivity analyses NS-1, 4, and 5 were used to explore the sensitivity of simulations to motion intensity. Sensitivity analyses NS-6 and NS-7 were used to assess the influence of superimposed ground motion high frequencies on simulation results. Table 27.5 presents the resulting horizontal displacement at the middle of the model surface and the duration of liquefaction at point P4 (P4 location: middle at 1-m depth) after the end of shaking.

Figure 27.11 presents a comparison of sensitivity analyses using PM4SAND in terms of excess pore pressure ratio, horizontal displacement time history and amplification ratio at the middle surface of the model for NS1, NS6, and NS7. Input ground motions for analyses NS6 and NS7 have superimposed high frequencies, and input motion NS7 is equal to input motion NS6 multiplied by 1.43. This figure indicates that superimposed high frequencies in the input ground motion as well as motion intensity can have a significant effect on the model response.

The predicted displacements were evaluated against various intensity parameters, and meaningful trends were discovered between permanent displacements and input ground motion Arias intensity. Figure 27.12 presents the predicted horizontal displacements at the middle surface of the models versus Arias intensity for sensitivity analyses with D_R of 65%. As expected, for higher Arias intensity motions, the predicted permanent displacements are higher. It appears that motions with high frequency content (NS-6 and NS-7) can result in greater displacements than motions with lower high frequency content and similar Arias intensity.

The sensitivity analyses also show that soil relative density has a significant impact on the model behavior.

Table 27.5 Sensitivity analyses: inputs and results

Simulation #		NS-1	NS-2	NS-3	NS-4	NS-5	NS-6	NS-7
Dry density (kg/m^3)		1651	1608	1683	1651	1651	1651	1651
Soil		Ottawa F65	Ottawa F65	Ottawa F65	Ottawa F65	Ottawa F65	Ottawa F65	Ottawa F65
D_R (assuming $p_{max} = 1765$ & $p_{min} = 1476$ kg/m^3)		65%	50%	75%	65%	65%	65%	65%
Motion to be used for simulation provided in Excel sheet		Achieved RPI-1, Motion 1	Anticipated RPI-3 Motion 1	Achieved RPI-1, Motion 1	Achieved RPI-1, Motion 1 scaled up	Achieved RPI-1, Motion 1 scaled down	Achieved RPI-2 Motion 1	Achieved RPI-2 Motion 1 scaled up
PGA (g)		0.15	0.15	0.15	0.25	0.11	0.14	0.2
PGA of 1 Hz component (g)		0.135	0.135	0.135	0.27	0.099	0.11	0.16
PGA of the high frequency component (g)		0.021	0.021	0.021	0.035	0.015	0.08	0.11
Simulation result: X-displacement at middle point on the specimen surface (cm)	PM4SAND	0.7	48	0	28.9	0.2	10.6	32.6
	UBCSAND	4.9	63.6	0.2	13.9	0.2	12.4	25.1
Simulation result: Duration of liquefaction at P4 after end of shaking (cm)	PM4SAND	0	130	0	80	0	20	60
	UBCSAND	0	0	0	0	0	0	0

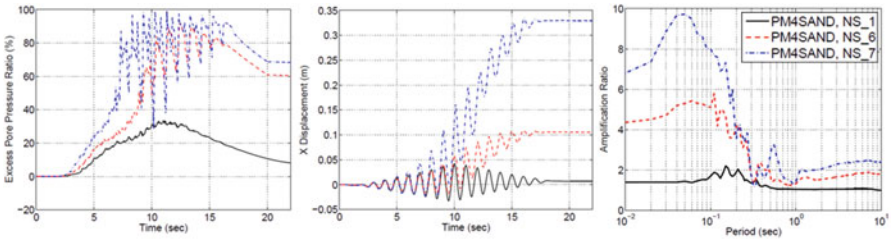

Fig. 27.11 Comparison of sensitivity analyses using PM4SAND in terms of excess pore pressure ratio, horizontal displacement time history and amplification ratio at the middle surface of the model for NS1, NS6, and NS7. (Input ground motions for analyses NS6 and NS7 have superimposed high frequencies. Input motion NS7 is input motion NS6 multiplied by 1.43)

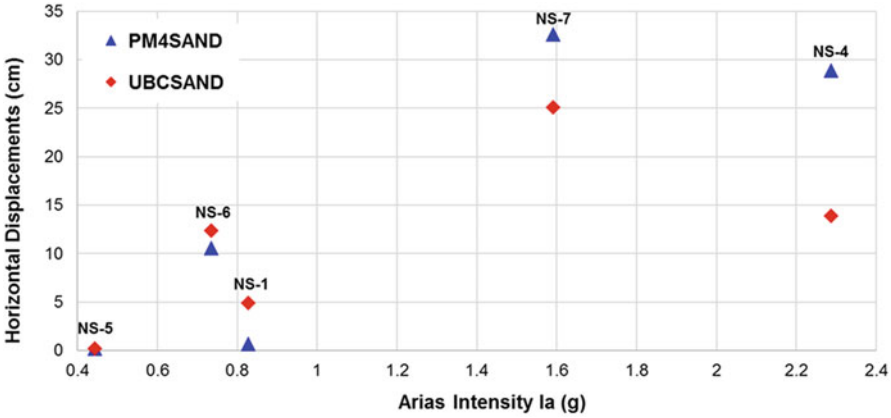

Fig. 27.12 Horizontal displacements at middle surface of the models versus Arias intensity for sensitivity analyses with D_R of 65%

27.6 Conclusions

We used two different constitutive models (PM4SAND and UBCSAND), implemented in the software FLAC, to simulate liquefaction-induced slope instability from six centrifuge tests.

The methodology adopted for the constitutive model calibration process considered both liquefaction triggering and post-liquefaction accumulation of shear strains. Firstly, constitutive models, PM4SAND and UBCSAND, were calibrated against laboratory tests to comply with liquefaction triggering criteria such as the number of cycles required to reach specific strain and pore pressure ratio thresholds. Secondly, the strain accumulation rate (SAR) following liquefaction triggering was used as a target for model parameter calibration.

Overall, the blind predictions captured the centrifuge tests behavior well and bounded the centrifuge response in most cases, indicating the benefits of using more than one constitutive model when performing numerical modeling. The predicted permanent displacements based on both constitutive models were generally within a factor of 2 from the actual measurements. The liquefaction strength curves implied by the UBCSAND model are steeper than the ones implied by PM4SAND and the laboratory test data. Hence, during the Type-C simulations, the UBCSAND model calibration was adjusted considering a CSR range corresponding to the CSR induced by the input motions. This should be considered when model calibrations are performed in practice, especially when multiple hazard levels are involved.

Differences between the predicted and measured responses are partially associated with limitations in the laboratory test data available, which affect the results of the numerical model calibration. For example, direct simple shear tests rather than triaxial tests, tests with static bias in addition to the no-bias conditions as well as tests at different CSR levels, representative of the CSR induced by the input motions, would be more relevant and are recommended. Differences between observed and computed responses are also attributed to simplifications in the prototype-scale numerical model (e.g., simulating possibly heterogeneous actual conditions with an idealized uniform relative density), accuracy of measurements and conversions from model to prototype scale, and differences between the input motions in the simulations ("average" of recorded at the centrifuge base) and the actual recorded input motions in the centrifuge which may vary across its base.

The sensitivity analyses suggest that horizontal displacements increase when high frequencies are introduced in the ground motion and for smaller soil relative density and higher ground motion intensity.

References

Beaty, M., & Byrne, P. M. (1998). An effective stress model for predicting liquefaction behavior of sand. In *Proceedings of a specialty conference, geotechnical earthquake engineering and soil dynamics* (pp. 766–777). Seattle: ASCE.

Boulanger, R. W., & Ziotopoulou, K. (2015). *PM4Sand (Version 3): A sand plasticity model for earthquake engineering applications. Technical Report No. UCD/CGM-15/xx, Center for Geotechnical Modeling*. Department of Civil and Environmental Engineering, University of California, Davis, CA

Byrne, P. M., Park, S. S., Beaty, M., Sharp, M., Gonzalez, L., & Abdoun, T. (2004). Numerical modeling of liquefaction and comparison with centrifuge tests. *Canadian Geotechnical Journal, 41*(2), 193–211.

El Ghoraiby, M. A., Park, H., & Manzari, M. T. (2017). *LEAP 2017: Soil Characterization and Element Tests for Ottawa F65 Sand*. Washington, DC: The George Washington University.

El Ghoraiby, M. A., Park, H., & Manzari, M. T. (2019). Physical and mechanical properties of Ottawa F65 sand. In B. Kutter et al. (Eds.), *Model tests and numerical simulations of liquefaction and lateral spreading: LEAP-UCD-2017*. New York: Springer.

Giannakou, A., Travasarou, T., Ugalde, J., Chacko, J., & Byrne, P. (2011). Calibration methodology for liquefaction problems considering level and sloping ground conditions. In *5th International Conference on Earthquake Geotechnical Engineering, Paper No. CMFGI, January*.

Itasca Consulting Group Inc. (2011). *Fast Lagrangian Analysis of Continua (FLAC2D)*. V. 7.0.
Itasca Consulting Group Inc. (2017). *Fast Lagrangian Analysis of Continua (FLAC2D)*. V. 8.0.
Marti, J., & Cundall, P. A. (1982). Mixed discretisation procedure for accurate solution of plasticity problems. *International Journal Numerical Methods and Analytical Methods in Geomechanics, 6*, 129–139.
Travasarou, T., Chen W. Y., & Chacko, J. (2011). Liquefaction-induced uplift of buried structures insights from the study of an immersed railway tunnel. In *5th International Conference on Earthquake Geotechnical Engineering, Paper No. LITUR, January*.